Free Form Deformations Guided by Gradient Vector Flow: A Surface Registration Method in Thoracic and Abdominal PET-CT Applications

Oscar Camara, Gaspar Delso, and Isabelle Bloch

Ecole Nationale Supérieure des Télécommunications
Département TSI, CNRS URA 820, 46 rue Barrault
75634 Paris Cedex 13, France
{Oscar.Camara,Gaspar.Delso,Isabelle.Bloch}@enst.fr

Abstract. A nonlinear surface registration algorithm of thoracic/abdominal structures segmented from CT and PET volumes is presented. The aim of this work is to develop a method that can provide an initial estimate of the elastic deformation between the images, so that MI-based techniques can be successfully applied. To perform the matching, a B-spline Free Form Deformation (FFD) model has been chosen. Hierarchical structure segmentation and rigid registration are applied to initialize the nonlinear surface registration phase. Two different approaches to optimize the warp are tested: an iterative gradient descent technique based on local gradient estimations over the grid of control points; and an original optimization based on Gradient Vector Flow (GVF) computed on the CT image. Finally, we evaluate our results, using an Iterative Closest Point (ICP) rigid registration algorithm as a reference to compare both approaches.

1 Introduction

Image registration is an image processing tool that can significantly improve clinical decisions in oncology applications. In this field, the need to combine anatomical and functional images is increasing, due to the development of new acquisition devices and methods that provide complementary information. Positron Emission Tomography (PET) acquisitions provide rich functional information for diagnostic and therapeutic follow-up of cancer, but make it difficult to precisely locate the tumors with respect to the surrounding anatomy. On the other hand, Computed Tomography (CT) and Magnetic Resonance Imaging (MRI) give access to this anatomical information, but do not offer sufficient data to state the lesion malignancy. Therefore, combining information from these two modalities would have a significant impact on improving medical decisions for diagnosis, therapy and treatment planning [1]. To perform such a combination, a registration step is needed in order to grant a good correspondence between the anatomical structures contained in the images.

In thoracic/abdominal oncology, the main problem to be solved to achieve the registration is to deal with the severe deformations undergone by the anatomical

structures of interest due to the different acquisition protocols involved, the elastic nature of the imaged regions and the patient's own metabolic activity. For this reason, linear transformations (rigid or affine) cannot be employed to model the deformation between both image modalities.

Several nonlinear transformations can be found in the image processing literature, such as thin-plate splines [2], elastic [3] and viscous fluid [4] models. However, our application imposes certain conditions: a high enough number of degrees of freedom to cope with large deformations; a limited computational cost to be able to use it in clinical routine; and the impossibility of employing external landmarks to help the registration procedure. B-Spline Free Form Deformations (FFD), introduced by Sederberg et al. [5], is a parametric technique which provides flexible nonlinear transformations which fulfill our needs.

FFD combined with Mutual Information (MI) criterion have been successfully used in different medical imaging applications, such as pre-and post contrast MR mammogram registration [6], brain registration [7] or cardiac segmentation [8]. Most of these applications work with monomodality data, where relationship between corresponding intensities in both images to register is simpler than in multimodality applications. That is not our case, as thoracic/abdominal PET and CT images show larger intensity differences between corresponding structures and a big deal of noise and artifacts, that can cause a MI-based algorithm to converge towards non optimal registration results.

One way to avoid this problem is to initialize these deformations close enough to the final solution, thus reducing the risk of falling into local minima. We have proved in [9] how this initialization can improve MI-based nonlinear registration results, this posterior phase being considered as a refinement step of the initialization results, capable of correcting any errors the segmentation might have induced and improving the registration of those regions distant from the segmented structures. In this article, we present an original nonlinear registration method between homologous structures segmented in both PET and CT images, to initialize the grey-level FFD-based multimodality registration. The main contribution of this paper, concerning the registration domain, is the use of a Gradient Vector Flow vector field computed on the CT structures to guide the FFD model applied on the PET objects.

The article is organized as follows. First, we describe the preprocessing stage including structure segmentation and the initial rigid registration. In Section 3, we present both FFD-based approaches to perform nonlinear surface registration. Comparative evaluation of the methods is discussed in Section 4 and, finally, conclusions are presented.

2   Preprocessing

2.1   Structure Segmentation

The registration step requires the segmentation of some common structures in both images. It is important to note that the quality of the segmentation does not need to be perfect, as the target is just to provide an initial estimate of the

Fig. 1. Left: 3D rendering of segmented structures in CT image superimposed on a coronal slice. Right: 3D rendering of segmented structures in PET image superimposed on a coronal slice.

transformation between these structures and errors induced by this stage will be corrected by the posterior grey-level registration phase. Working with several clinicians, we have determined a list of structures that can always be found in thoracic/abdominal PET and CT images. For the time being, we have worked with the three most relevant organs: lungs, liver and kidneys. Segmentation of these anatomical features is not a trivial task, especially in PET scans, where gradients are weak and sometimes the poor image quality does not allow to recognize even visually the different structures.

Due to the above reasons, we propose a hierarchical procedure: the extraction of a given structure will be driven by information derived from a simpler one. This information is composed both of spatial constraints and relationships inferred from the previously segmented structures, expressed by means of Regions Of Interest (ROI) in which the search for new structures will take place. The order in which structures are segmented is: body contours, lungs, kidneys and liver. Some results of the final segmentation are shown in Figure 1.

Each structure is processed in two different stages: a first rough segmentation and a refinement of the result. Rough segmentation is basically composed of automatic thresholding and mathematical morphology operations in the ROI defined by previously segmented objects. Some properties of the images and of the anatomy are exploited in order to make this phase more robust, especially in PET images:

– PET lungs: PET acquisition often provides emission and transmission images, the lungs being easier to segment in the latter. We perform lung segmentation in the transmission image to initialize the segmentation in the emission image, thus improving the quality and the robustness of the results.

- Kidneys: These structures are segmented by selecting the two most symmetrical components with respect to the body's symmetry plane. The symmetry plane computation and the selection of symmetrical regions are made using an algorithm and a symmetry measure proposed in [10].
- Liver: Often, the liver is much easier to segment in one modality than in the other. In those cases, we roughly register segmented structures from one modality to the other and dilate them to produce a ROI, which restricts the search in the more difficult images.

The results obtained from the previous stage cannot be considered as a final result. In particular, the lack of a regularization term may lead to imperfect boundaries. These problems are overcome using a 3D simplex mesh deformable model [11].

2.2   Rigid Surface Registration

Once the organs are conveniently segmented, they can be easily used to automatically establish a first approximation of the registration. It includes a rigid motion, independent scaling along the three axes and cropping out those parts of the volumes without a correspondence or that have no interest for our application.

3   Nonlinear Surface Registration

The registration of 3D surfaces has been extensively treated in various fields of image processing and computer vision. Interesting reviews of these techniques can be found in [12] [13].

One of the most successful methods is the Iterative Closest Point (ICP), proposed by Besl et al. [14], and it has been widely used with good results in several applications. This algorithm iteratively tunes a rigid transformation to minimize the distance between two point (line, triangle, ...) sets whose correspondences have been determined by proximity. In previous works [9], we have employed the distance map computed for this method to perform an estimation of the nonlinear transformation between the surfaces of each pair of organs. This was used to initialize the positions of the control points of the FFD of the grey-level MI registration stage. Nevertheless, this method presented some problems, such as erroneous deformations around those structures without an obvious correspondence. Furthermore, the interaction with FFD-based grey-level registration was solved in a way where some information could be lost.

For these reasons, we have chosen to apply to this surface registration stage the same FFD deformation framework used in the grey-level registration stage, simplifying the interaction between both phases. In this section, after a brief introduction to the FFD model, we propose two FFD-based approaches to achieve nonlinear surface registration. The first method employs a Root Mean Square (RMS) criterion as a similarity measure, computing a local estimation of the gradient at each control point of the grid, and using an iterative gradient descent

procedure. The second method computes a Gradient Vector Flow (GVF) field over CT segmented structures to guide the optimization of the control points.

3.1   Free Form Deformation Model

In this technique, deformations of the object are achieved by tuning an underlying mesh of control points, which in the present application has been set to $10 \times 10 \times 10$ effective nodes. The control point displacements are then interpolated to obtain a smooth and continuous C^2 transformation. A B-Spline based FFD can be written as a 3D tensor product of one-dimensional cubic B-Splines. Let Φ denote an uniformly spaced grid of $n_x \times n_y \times n_z$ control points $\phi_{i,j,k}$ with a spacing of δ, where $-1 \leq i < n_x - 1, -1 \leq j < n_y - 1, -1 \leq k < n_z - 1$. Then, the nonlinear displacement field for each image point x,y,z is computed:

$$d(x, y, z) = \sum_{l=0}^{3} \sum_{m=0}^{3} \sum_{n=0}^{3} \theta_l(u)\theta_m(v)\theta_n(w)\phi_{i+l,j+m,k+n} \tag{1}$$

Here, i, j, and k denote the indices of the control point cell containing (x,y,z), and u, v, and w are the relative positions of (x,y,z) in the three dimensions, θ_0 through θ_3 being 1D cubic B-Splines.

3.2   Free Form Deformations Guided by Root Mean Square (RMS-FFD)

We have to chose a similarity criterion to control the optimization of the FFD grid of control points. Segmented images have a linear intensity relation, thus the simpler way is to employ the Root Mean Square (RMS) difference of corresponding pixels intensities. We could use other simpler similarity measures but we have chosen the RMS in order to deal with several structures in each image at the same time, as it is planned in future works.

The optimization procedure is based on an iterative gradient descent technique over the entire grid of control points. At each iteration, we compute a finite differences local gradient estimation for each control point. Furthermore, a local spring force regularization term, pulling each node towards the centroid of its neighbouring nodes, has been added to avoid overfitting and to prevent the nodes from intersecting, which could lead to unwanted alterations of the structure topology. Results of this method applied to the lungs and liver are shown in Figure 2, where the good performance of this nonlinear registration algorithm can be appreciated.

3.3   Free Form Deformations Guided by Gradient Vector Flow (GVF-FFD)

A drawback of the RMS-FFD method is the need to optimize all the control points with the local gradient estimation computed at each iteration. Multi-resolution approaches accelerate the convergence of the algorithm, but the gradient estimation remains a problem in terms of computation time.
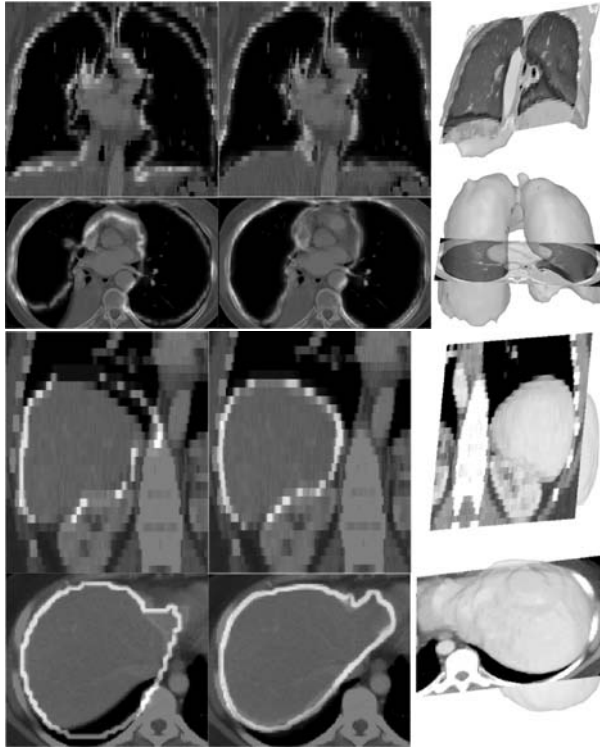
Fig. 2. Original coronal and axial CT slices are superimposed with: Left: contour of rigidly registered PET structures; Center: contour of PET structures nonlinearly registered with RMS-FFD method; Right: 3D rendering PET structures nonlinearly registered with RMS-FFD method. 3D images shown in this article have been visualized using the Anatomist software (www.anatomist.info), developed at S.H.F.J, Orsay.

We propose an original way to speed-up the optimization of the deformation, computing a vector field over the target structures (in our case, those segmented from the CT images) to guide the tuning of the Free Form Deformation applied to the source structures (in our case, those segmented from the PET images).

Gradient Vector Flow, proposed by Xu et al. [15], is an elegant method to obtain this vector field, giving us at each image point the direction towards the target anatomical feature. This technique is usually used to guide deformable models in segmentation applications, but to our knowledge, it has not been used before to control FFD in registration algorithms.

A GVF field $\mathbf{v}$ is defined as the equilibrium solution of the following vector diffusion equation:

$$\mathbf{u}_t = g(|\nabla f|)\nabla^2 \mathbf{u} - h(|\nabla f|)(\mathbf{u} - \nabla f) \tag{2}$$

$$\mathbf{u}(x,0) = \nabla f(x) \tag{3}$$

where $f(x)$ has been obtained applying a Canny edge detector to the target image. The first term at the right side of equation (2) is called *smoothing term*, and tends to uniformize the resulting vector field. The second term is the *data term*, and drives the vector field u towards the $\triangledown f$ computed from the data. $g()$ and $h()$ are weighting functions that apply respectively to the smoothing and data term. A common choice for these is:

$$g(|\triangledown f|) = e^{-\left(\frac{|\triangledown f|}{K}\right)^2}, \qquad h(|\triangledown f|) = 1 - g(|\triangledown f|) \qquad (4)$$

This formulation allows for the gradient vector diffusion only where there are no strong edges, thus preventing the smoothing effect from averaging close opposing gradients, which could lead to a gap in the contour through which our model could leak.

After the computation of the GVF vector field, we have for each point belonging to a PET structure the right direction to evolve towards its corresponding CT structure. Thus, for each grid control point, we find the contour points of the PET structures under its influence and we observe the value of GVF vector field for these points. These values are weighted according to their grid control point and the mean of the resulting vectors is taken as the optimal control point displacement direction. At the end of each iteration, a local spring regularization term is applied like in the RMS-FFD algorithm.

The convergence of the algorithm depends on the quality of the computed vector field. Moreover, control points tend to oscillate in the vicinity of CT structure boundaries. Therefore, several constraints over the control points have been implemented to stop them when they start to oscillate. We have introduced the procedure in a multi-step framework to help the algorithm to cope with large deformations in the first iterations, leaving more local ones at the end. Results of this method applied to the lungs and the liver structures are shown in Figure 3. We can appreciate that we obtain lower quality deformations with respect to the RMS-FFD method. On the other hand, this algorithm converges much faster towards correct transformations, as we show in Section 4.

4   Comparison of the Methods

In this section, we compare quantitatively the quality and computational cost the two proposed FFD-methods compared to the ICP algorithm. We have applied these techniques over a database composed of 15 pairs of deformable structures, such as lungs, liver or kidneys, previously segmented from CT and PET images.

To evaluate quality other than by visual inspection of 3D volumes, we have computed two quantitative measures: an overlap measure directly applied on the segmented structures and the Mutual Information (MI) applied on the grey-level intensity images. The reason of using MI instead of RMS directly over segmented structures is to take into account the possible errors induced by the segmentation phase.

The overlap measure consists of the quotient between intersection and union among segmented structures, and is equal to 1 if total superimposition is
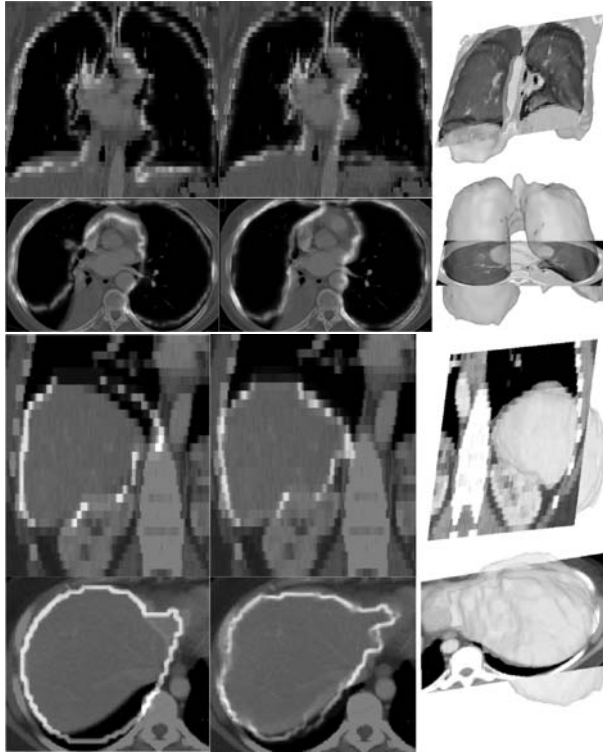
Fig. 3. Original coronal and axial CT slices are superimposed with: Left: contour of rigidly registered PET structures; Center: contour of PET structures nonlinearly registered with GVF-FFD method; Right: 3D rendering PET structures nonlinearly registered with GVF-FFD method.

achieved. Mutual Information (MI) criterion, introduced by Viola [16], is a powerful tool for multimodal image registration with nonlinear intensity relation. It expresses how much information from an image I is contained in another image J. Therefore, MI will be maximal if the images are geometrically aligned. Thus, we compute MI between grey level CT image and grey-level PET image, registered by applying the FFD computed over the surfaces. Table values of the overlap measure and MI are completed with the improvement percentage respect to the ICP results.

Furthermore, we have analyzed the computational costs of each method. We have normalized the results by the dimensions of each image, to be able to compare directly method performances, independently of the registered structures. Thus, table values of time are in μs./pixel. Quantitative results and computational costs are summarized in Table 1.

The overlap measure and MI confirm the visual results, that is, RMS-FFD is the method which obtains the best deformations, while GVF-FFD still clearly surpasses rigid registration methods. It is worth noticing how the overlap of the

Table 1. Evaluation results.

Method	ICP	RMS-FFD	GVF-FFD
Overlap(value/%)	0.6586/100	0.9030/137.095	0.8275/122.081
MI(value/%)	0.1888/100	0.2592/137.286	0.2486/131.697
Time	6.60723	699.365	52.610

segmented structures never reaches 100 %; this is due to the inherent regularization of the chosen elastic deformation model, which prevents the finer differences from being removed. As a matter of fact this is quite convenient, because those differences are usually due to the imaging modalities involved rather than to misregistration, and must be preserved as they are.

We have observed that RMS-FFD works better than GVF-FFD in regions with very small deformations. This is due to the trade-off in the computation of the GVF vector field between the rejection of undesired structures, such as bronquia in the case of lungs, and the capacity to cope with local deformations.

On the other hand, GVF-FFD shows better performance in terms of rapidity of convergence, while RMS-FFD remains a high-computational cost algorithm, due to the computation of local gradient estimations in each iteration. We have tried initializing RMS-FFD with the solution furnished by the GVF-FFD, obtaining even better quality results than using only RMS-FFD, while having acceptable convergence times.

5   Conclusions

We have proposed an original nonlinear surface registration framework based on a FFD model applied to segmented structures from thoracic/abdominal CT and PET images, aimed at initializing a posterior grey-level MI nonlinear registration algorithm. Two different approaches to optimize the deformation, RMS-FFD and GVF-FFD have been presented. A quantitative evaluation of these methods compared to the classical ICP algorithm has been performed. RMS-FFD has proved to be the method providing best results in terms of registration quality, at the expense of a high computational cost. On the other hand, GVF-FFD, furnishing slightly less accurate deformations, converges towards the solution in a much shorter time.

Acknowledgment

References

1. H. N. Wagner, "Fused Image Tomography: An Integrating Force," *Nuclear Medicine*, vol. 40, no. 8, pp. 13N–32N, 1999.
2. F. Bookstein, "Principal warps: Thin-plate splines and the decomposition of deformations," *IEEE Transactions on Pattern Analysis and Machine Intelligence*, vol. 11, no. 6, pp. 567–585, 1989.
3. R. Bajcsy and S. Kovacic, "Multiresolution elastic matching," *Computer Vision, Graphics and Image Processing*, vol. 46, pp. 1–21, 1989.
4. M. Bro-Nielsen and C. Gramkow, "Fast fluid registration of medical images," in *VBC*, Hamburg, Germany, Sept. 1996, pp. 267–276.
5. T. Sederberg and S. Parry, "Free form deformation of solid geometric models," in *SIGGRAPH'86*, vol. 20, Dallas, USA, August 1986, pp. 151–160.
6. D. Rueckert, I. Somoda, C. Hayes, D. Hill, M. Leach, and D. Hawkes, "Nonrigid Registration Using Free-Form Deformations: Applications to Breast MR Images," *IEEE Transactions on Medical Imaging*, vol. 18, no. 8, pp. 712–721, 1999.
7. T. Hartkens, D. Hill, A. Castellano-Smith, D. Hawkes, C. M. Jr., A. Martin, W. Hall, H. Liu, and C. Truwit, "Using points and surfaces to improve voxel-based non-rigid registration," in *MICCAI*, 2002, pp. 565–572.
8. J. Lotjonen, "Segmentation of mr images using deformable models: Application to cardiac images," *International Journal of Bioelectromagnetism*, vol. 3, no. 2, pp. 37–45, 2001.
9. O. Camara, G. Delso, and I. Bloch, "Evaluation of a thoracic elastic registration method using anatomical constraints in oncology," in *EMBS-BMES'02*, Houston, USA, October 2002.
10. O. Colliot, I. Bloch, and A. Tuzikov, "Characterization of approximate plane symmetries for 3D fuzzy objects," in *IPMU*, vol. 3, Annecy, France, July 2002, pp. 1749–1756.
11. H. Delingette, "General object reconstruction based on simplex meshes," *International Journal of Computer Vision*, vol. 32, no. 2, pp. 111–146, 1999.
12. M. Audette, F. Ferrie, and T. Peters, "An algorithmic overview of surface registration techniques for medical imaging," *Medical Image Analysis*, vol. 4, pp. 201–217, 2000.
13. J. B. A. Maintz and M. A. Viergever, "A Survey of Medical Image Registration," *Medical Image Analysis*, vol. 2, no. 1, pp. 1–36, 1998.
14. P. Besl and N. McKay, "A method for registration of 3D shapes," *IEEE Transactions on Pattern Analysis and Machine Intelligence*, vol. 18, no. 14, pp. 239–256, 1992.
15. C. Xu, "Deformable models with application to human cerebral cortex reconstruction in magnetic resonance images," Ph.D. dissertation, Johns Hopkins University, 2000.
16. P. Viola, "Alignment by maximization of mutual information," Ph.D. dissertation, MIT, Cambridge, Ma, 1995.